CHEMISTRY
A EUROPEAN JOURNAL

DOI: 10.1002/chem.200701740

A Radical-Anion Chain Mechanism Initiated by Dissociative Electron Transfer to a Bicyclic Endoperoxide: Insight into the Fragmentation Chemistry of Neutral Biradicals and Distonic Radical Anions

David C. Magri*[a] and Mark S. Workentin*[b]

Dedicated to the memory of Professor Yoshihiro Matsumura in honour of his outstanding contributions to the fields of synthetic chemistry and electro-organic chemistry

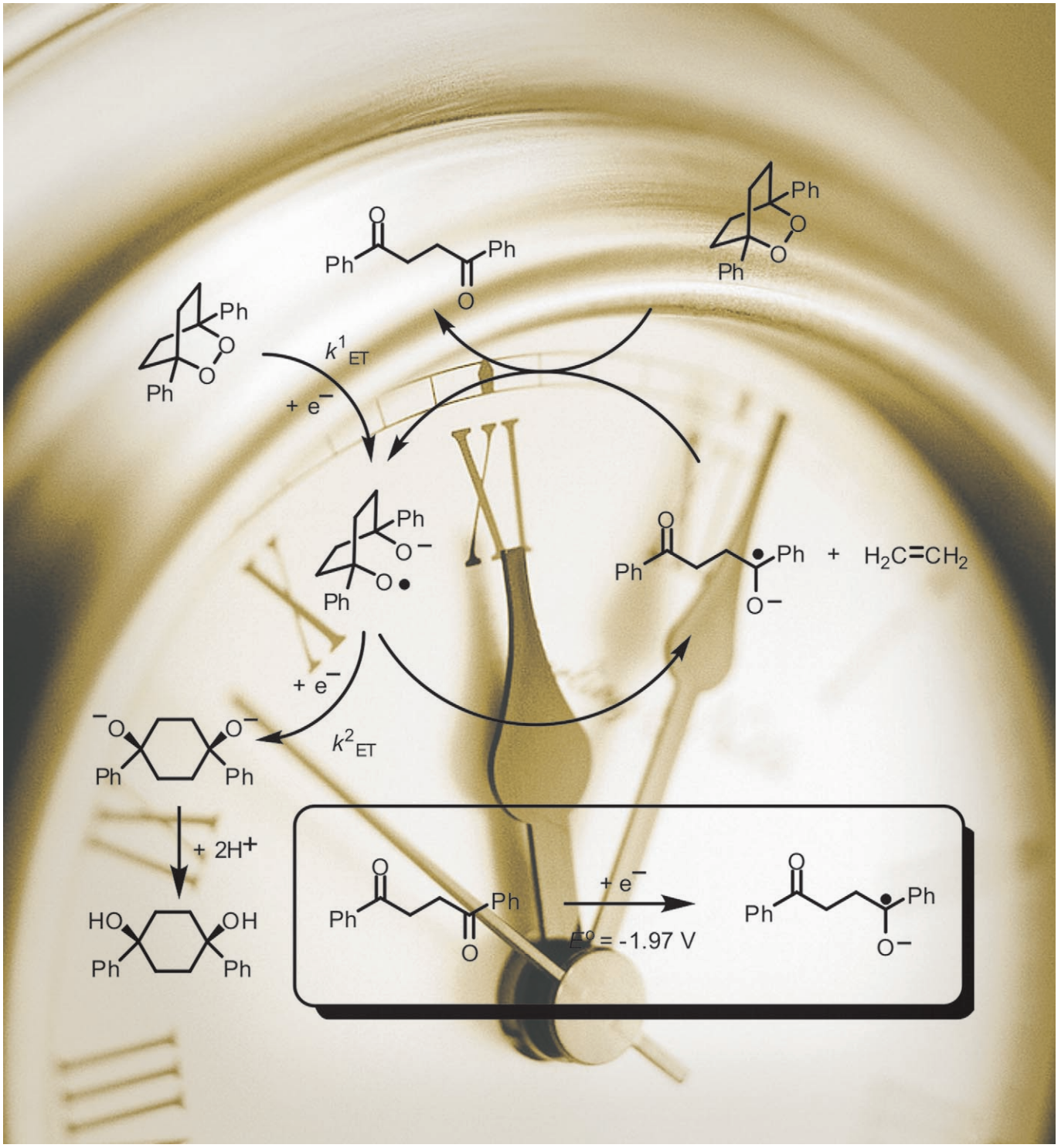

Abstract: The electron-transfer (ET) reduction of two diphenyl-substituted bicyclic endoperoxides was studied in *N*,*N*-dimethylformamide by heterogeneous electrochemical techniques. The study provides insight into the structural parameters that affect the reduction mechanism of the O–O bond and dictate the reactivity of distonic radical anions, in addition to evaluating previously unknown thermochemical parameters. Notably, the standard reduction potentials and the bond dissociation energies (BDEs) were evaluated to be -0.55 ± 0.15 V and 20 ± 3 kcal mol^{-1}, respectively, the last representing some of the lowest BDEs ever reported. The endoperoxides react by concerted dissociative electron transfer (DET) reduction of the O–O bond yielding a distonic radical-anion intermediate. The reduction of 1,4-diphenyl-2,3-dioxabicyclo[2.2.2]oct-5-ene (**1**) results in the quantitative formation of 1,4-diphenylcyclohex-2-ene-*cis*-1,4-diol by an overall two-electron mechanism. In contrast, ET to 1,4-diphenyl-2,3-dioxabicyclo[2.2.2]octane (**2**) yields 1,4-diphenylcyclohexane-*cis*-1,4-diol as the major product; however, in competition with the second ET from the electrode, the distonic radical anion undergoes a β-scission fragmentation yielding 1,4-diphenyl-1,4-butanedione radical anion and ethylene in a mechanism involving less than one electron. These observations are rationalized by an unprecedented catalytic radical-anion chain mechanism, the first ever reported for a bicyclic endoperoxide. The product ratios and the efficiency of the catalytic mechanism are dependent on the electrode potential and the concentration of weak non-nucleophilic acid. A thermochemical cycle for calculating the driving force for β-scission fragmentation is presented, and provides insight into why the fragmentation chemistry of distonic radical anions is different from analogous neutral biradicals.

Keywords: electron transfer · fragmentation · peroxides · radical ions · reactive intermediates

Introduction

Radical anions have emerged as an important class of reactive intermediate in various bioorganic processes.[1] They result from the transfer of a single electron to a neutral molecule to yield an intermediate possessing both a charge and radical character. In the past, it has often been assumed that the reactivity of radical anions, in particular for fragmentation and rearrangement reactions, was similar to neutral radicals. Recent research, notably by Tanko and co-workers, has shown that this assumption is not valid as both charge and spin are governing factors in the reactivity of radical-anion rearrangements.[2,3] There are a number of examples involving the rearrangements of radical anions in which bond cleavage results in formation of a single species containing a spatially separated radical and anion [Eq. (1)].[2–5] However, examples involving the fragmentation of a spatially separated radical anion yielding a localized radical anion and a neutral molecule are rather unknown [Eq. (2)].

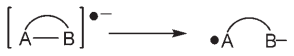

(1)

(2)

Using primarily electrochemical techniques, we have been studying the electron-transfer (ET) reduction of organic endoperoxides.[6–12] These studies have not only provided previously unknown kinetic and thermochemical data, but also an insight into the reactivity of distonic radical anions, a reactive intermediate containing a spatially separated alkoxyl radical and alkoxyl anion. Initial studies focused on the dialkyl-substituted bicyclic endoperoxides, ascaridole (ASC) and dihydroascaridole (DASC),[6,7] and on the antimalarial drug, artemisinin (ART).[8,9] These studies revealed that ET

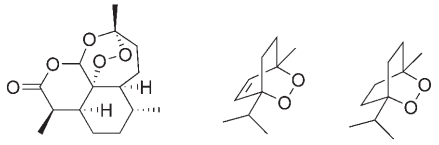

to the O–O bond occurs by a *concerted* dissociative reductive mechanism [Eqs. (3) and (4)]. Upon ET, the incoming electron is accepted into a σ* orbital associated with the O–O bond, which concomitantly cleaves to generate the distonic radical anion [Eq. (3)]. With these bicyclic endoperoxides, the distonic radical anion was found to be subsequently reduced at the electrode in a second heterogeneous ET resulting in quantitative formation of the *cis*-diols [Eq. (4)].[6,7]

[a] Dr. D. C. Magri
Faculty of Science
University of Ontario Institute of Technology
2000 Simcoe Street North, Oshawa, Ontario L1H 7K4 (Canada)
Fax: (+1) 905-721-3304
E-mail: david.magri@uoit.ca

[b] Prof. Dr. M. S. Workentin
Department of Chemistry
The University of Western Ontario, London
Ontario N6A 5B7 (Canada)
Fax: (+1) 519-661-3022
E-mail: mworkent@uwo.ca

Supporting information for this article is available on the WWW under http://www.chemeurj.org/ or from the author.

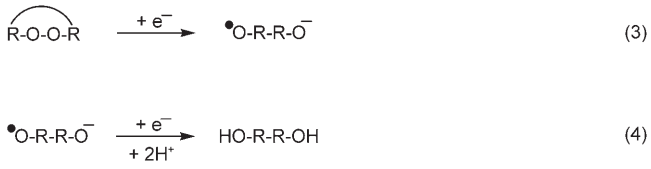

Subsequent electrochemical studies have been performed to investigate the ET reactivity of various diphenyl-substituted endoperoxides.[10–12] In these studies, it was discovered that the distonic radical anion can undergo a fragmentation in competition with the second heterogeneous ET [Eq. (3)]. These discoveries have provided the opportunity to gain further insight into the reactivity of these interesting reactive intermediates, and to exploit the competing fragmentation reaction in order to probe the rate constant of the second heterogeneous ET.[10,13] In the case of the anthracene-based endoperoxide, 9,10-diphenyl-9,10-epidioxyanthracene (DPA-O_2), a rapid 1,2-phenyl migration (*O*-neophyl-type rearrangement) was observed to compete with reduction from the electrode to yield another distonic radical anion with a carbon-centered radical that was subsequently reduced.[10,11] In another example, a β-scission fragmentation was observed from the distonic radical anion of 3,3,6,6-tetraphenyl-1,2-dioxane (TPD), to yield a localized radical anion and two neutral molecules. The preference for a β-scission fragmentation was partially rationalized due to the increased flexibility in the monocyclic structure.[12]

We now know of at least three competing processes available to the distonic radical anion generated electrochemically from the ET reduction of an endoperoxide: reduction, β-scission fragmentation, and *O*-neophyl-type rearrangement. In the studies of the rigid bicyclic endoperoxides ASC, DASC, and ART with alkyl bridgehead substituents, only reduction of the distonic radical anion was observed to yield the corresponding *cis*-diol [Eq. (4)]. However, with endoperoxides with phenyl substituents, as with DPA-O_2 and TPD, a fragmentation pathway is observed in competition with reduction from the electrode. While our understanding of distonic radical-anion fragmentations is improving, there is still a lack of fundamental information for predicting the reactivity pathway and for establishing activation/driving force relationships.[4] Among the many findings in this study, we highlight that the incorporation of phenyl substituents is not the only criteria for observing a competing fragmentation reaction from the distonic radical anion of a bicyclic endoperoxide.

We report the heterogeneous ET reduction of the bicyclic diphenyl-substituted endoperoxides 1,4-diphenyl-2,3-dioxabicyclo[2.2.2]oct-5-ene (**1**) and 1,4-diphenyl-2,3-dioxabicyclo[2.2.2]octane (**2**) (shown in Scheme 1). These endoperoxides were studied by using electrochemical techniques, including cyclic voltammetry and preparative electrolyses, to gain insight into the structural parameters that affect the reduction mechanism of the O–O bond and dictate the reactivity of distonic radical anions, in addition to evaluating previously unknown thermochemical parameters.

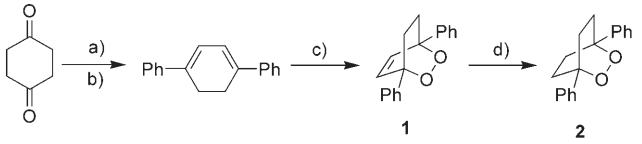

Scheme 1. The synthetic route and conditions used in the synthesis of the diphenyl-substituted endoperoxides **1** and **2**. a) PhLi, THF, −78 °C; b) TsOH, Δ, benzene; c) O_2, MTTP, *hv*, 1:1 benzene/CH_2Cl_2; d) N_2H_2, CH_2Cl_2.

We report that the slight modification in the molecular structure between **1** and **2** has a dramatic effect on the reactive pathways available to the resulting distonic radical anion. In contrast to DPA-O_2 and TPD, fragmentation is not observed from the distonic radical anion originating from **1**. However, the distonic radical anion from **2** undergoes a β-scission fragmentation that competes with reduction from the electrode [Eq. (2)]. Consequently, these reactive intermediates can be exploited as kinetic probes, or "molecular clocks", for estimating the heterogeneous ET to the distonic radical anions. We also provide insight into the structure–reactivity trends of oxygen-centered biradicals and analogous distonic radical anions. Moreover, the β-scission fragmentation initiates an unprecedented propagating radical-anion chain mechanism, the first ever reported from the concerted DET reduction of a bicyclic endoperoxide.

Results and Discussion

Synthesis: The synthesis of the diphenyl-substituted bicyclic endoperoxides, **1** and **2** began with the reaction of phenyllithium (PhLi) in tetrahydrofuran (THF) with cyclohexadione to yield a diastereomeric mixture of 1,4-diphenylcyclohexane-1,4-diol. The diol mixture was dehydrated to yield 1,4-diphenyl-1,3-cyclohexadiene by refluxing in benzene in the presence of excess *p*-toluenesulfonic acid (TsOH), and purified by flash chromatography, followed by recrystallization from hexanes. Endoperoxide **1** was prepared by photo-oxygenation of 1,4-diphenylcyclohexa-1,3-diene by irradiating O_2 saturated solutions of 1:1 benzene/dichloromethane containing a catalytic amount of *meso*-tetraphenylporphyrin (MTTP).[14,15] The saturated endoperoxide **2** was prepared from **1** by reduction with excess diimide generated in situ from potassium azodicarboxylate in the presence of acetic acid and then recrystallized.[16,17] Both endoperoxides were isolated as crystalline white solids. An outline of the synthetic route used to prepare the endoperoxides is summarized in Scheme 1.

Cyclic voltammetry: The electrochemical reduction of the diphenyl-substituted endoperoxides **1** and **2** was studied by cyclic voltammetry by using a glassy carbon electrode in *N*,*N*-dimethylformamide (DMF) containing 0.10 M tetraethylammonium perchlorate (TEAP). Cyclic voltammetry of **1** as shown in Figure 1 is characterized by a broad and electrochemically irreversible cathodic peak at all scan rates inves-

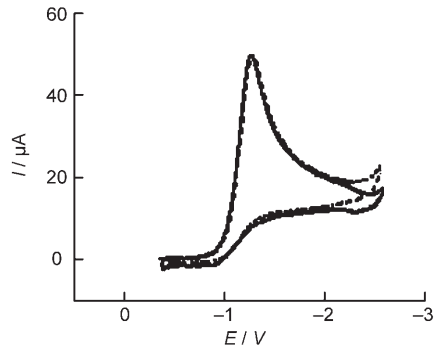

Figure 1. Cyclic voltammograms of 1.8 mM of **1** in DMF containing 0.10 M TEAP in the absence (solid line) and presence (dashed line) of five equivalents of 2,2,2-trifluoroethanol at 0.1 $V s^{-1}$.

tigated in the range 0.05–50 $V s^{-1}$. The peak potential (E_p) at 0.1 $V s^{-1}$ is located at −1.27 V versus SCE. Upon increasing the scan rate (ν) the E_p is found to shift negatively by 118 mV per log decade, and the cathodic wave broadens from 136 to 187 mV over the range 0.1–10 $V s^{-1}$. From the analysis of the peak widths, the transfer coefficient $\alpha = 1.857\,RT/(F\Delta E_{p/2})$ is found to decrease from 0.35 at 0.1 $V s^{-1}$ to 0.24 at 10 $V s^{-1}$. From the scan-rate dependence of the peak potential and $\alpha = 1.15\,RT/[dE_p/(d(\log \nu)]$, an average α of 0.25 is determined, which is consistent with a concerted dissociative ET mechanism ($\alpha \ll 0.5$).[18] On scanning back after the forward reduction in the positive direction, a poorly defined anodic peak is observed from the oxidation of the dialkoxide anion at about −0.2 V versus SCE.[6]

The voltammetry of **2** as shown in Figure 2 also exhibits a broad and irreversible wave with the E_p at −1.5 V, which is shifted negatively by 170 mV compared to **1**. This difference narrows on increasing the scan rate. The average α value of 0.28 indicates that the O−O reduction of **2** is also consistent with a concerted dissociative mechanism. Table 1 summarizes the voltammetry analysis of the dissociative wave for each endoperoxide. In contrast to **1**, beyond a switching potential of −2.0 V, the dissociative wave of **2** displays non-

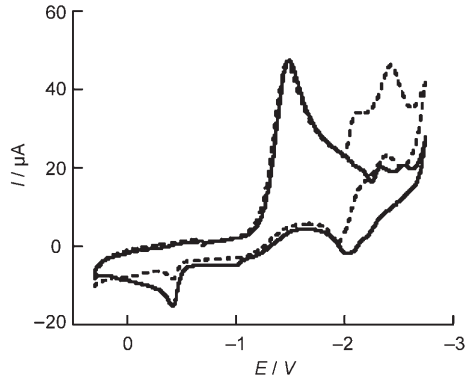

Figure 2. Cyclic voltammograms of 1.7 mM of **2** in DMF containing 0.10 M TEAP in the absence (solid line) and presence (dashed line) of five equivalents of 2,2,2-trifluoroethanol at 0.1 $V s^{-1}$.

Table 1. Cyclic voltammetry data for the dissociative ET reduction of diphenyl-substituted bicyclic endoperoxides in solutions of 0.10 M TEAP/DMF at 25 °C measured with a glassy carbon electrode.

	ν [$V s^{-1}$]	**1**	**2**
E_p [V][a]	0.1	−1.27	−1.45
	1.0	−1.37	−1.54
	10	−1.49	−1.64
$\Delta E_{p/2}$ [mV]	0.1	136	142
	1.0	150	151
	10	187	181
$\alpha = 1.857\,RT/(F\Delta E_{p/2})$	0.1	0.351	0.336
	1.0	0.318	0.316
	10	0.239	0.264
$\alpha = 1.15\,RT/F[dE_p/d(\log \nu)]$[b]		0.25	0.28
$dE_p/d(\log \nu)$ [mV^{-1}][b]		−118	−105
$n@E_p$ (no acid)		1.98	1.94
$n@E_p$ (acid)[c]		2.08	1.96
n@−2.5 V (no acid)		1.96	0.6

[a] Potentials are referenced versus ferrocene (0.475 V) versus SCE. [b] Based on scan rates between 0.1 and 10 $V s^{-1}$. [c] In the presence of 10 mM trifluoroethanol.

Cottrell behavior. The tail end of the dissociative wave, which is normally dictated exclusively by diffusion, displays an unusual oxidative dip. This feature of the voltammograms is most noticeable at slower scan rates as observed in Figure 2 at 0.1 $V s^{-1}$. Following the dip, two small irreversible cathodic peaks are also observed. On the reverse scan, an oxidation wave is detected in the proximity of −2 V. Scanning further in the positive direction reveals other oxidation waves within the general potential region between −0.8 and 0.2 V. Repetitive cycling voltammetry was used to probe the peaks in the vicinity of the dip. The voltammograms obtained at a scan rate of 1.0 $V s^{-1}$ are illustrated in Figure 3. At this scan rate, the dip is not observed after the

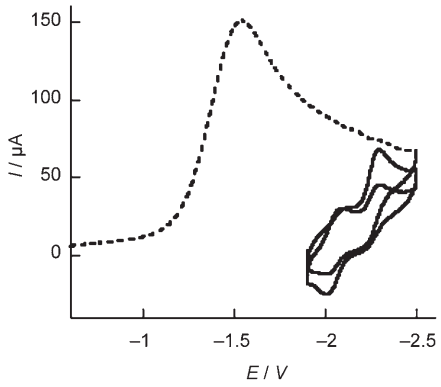

Figure 3. Cyclic voltammogram of 2.0 mM of **2** at 1.0 $V s^{-1}$. The dashed line corresponds to the initial reduction of the endoperoxide, and the solid line to repetitively cycling through the electroactive redox couples twice between the switching potentials of −1.9 and −2.5 V.

dissociative wave. However, two redox couples are observed at −1.98 and −2.20 V versus SCE, which correspond to electrochemically active species resulting from some reactivity of the distonic radical anion other than reduction by the electrode.

The electrochemical behavior of the endoperoxides was examined in the presence of weak non-nucleophilic acids and representative voltammograms are illustrated as dashed lines in Figures 1 and 2. In the presence of ten equivalents of excess 2,2,2-trifluoroethanol (TFE) or acetanilide, the peak width at half height, $\Delta E_{p/2} = E_{p/2} - E_p$, and peak height ($I_p$) for the dissociative wave of both **1** and **2** remain unaffected. The absence of any change in the dissociative wave is expected in concerted dissociative O–O bond reduction.[6,19] Also characteristic in the presence of excess weak acid is the disappearance of the anodic peaks normally observed in dry solvent at −0.3 V versus SCE at 0.1 V s^{-1}, which are attributed to the oxidation of the dialkoxide generated from the reduction of the endoperoxide. In the case of **2**, the cathodic peaks negative to the dissociative wave increase in current and shift in the positive direction. Most intriguing, the dip observed after the dissociative wave is absent on addition of a weak acid.

Constant potential electrolyses: Electrolysis experiments were performed to determine the reduction products and the electron stoichiometry (n) as a function of electrode potential and presence of weak acid. The results from the coulometry experiments obtained with a glassy carbon rotating disk electrode are included in Table 1. A summary of the products and the relative amounts isolated at different experimental conditions are shown in Scheme 2. Electrolyses

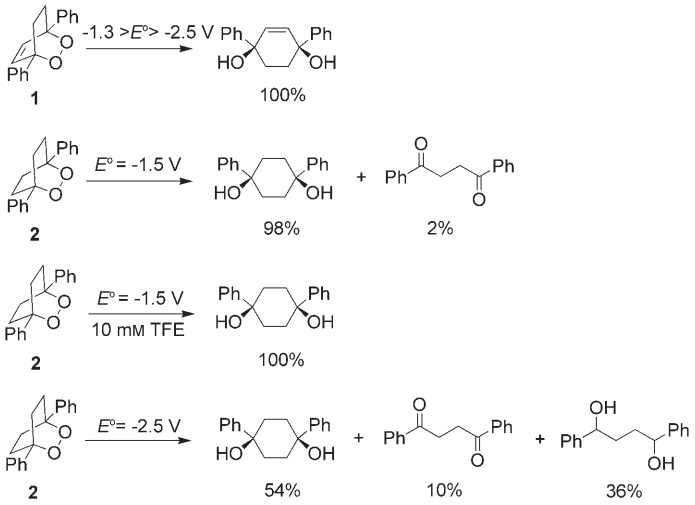

Scheme 2. The reduction products for **1** and **2** at different experimental conditions.

of **1** at potentials between −1.3 and −2.5 V results in the consumption of 2 F mol^{-1}, or two electron equivalents of charge, independent of the applied potential and the presence of a weak non-nucleophilic acid. No electroactive products were observed. Workup of the electrolyzed solution revealed the quantitative formation of the *cis*-diol, 1,4-diphenylcyclohex-2-ene-1,4-diol, which was fully characteristized (see Experimental Section). The diagnostic signals in the ^{1}H NMR spectrum were a sharp singlet at $\delta = 6.08$ ppm and a broad peak at $\delta = 1.61$ ppm corresponding to the alkene and the alcohol protons, respectively.

Electrolyses of **2** at the dissociative wave between the potentials of −1.4 and −1.7 V in the absence or presence of weak acid also results in the consumption of 2 F mol^{-1} of charge. In the absence of weak acid 1,4-diphenylcyclohexane-1,4-*cis*-diol accounted for 98% of the recovered mass, the other 2% was identified as 1,4-diphenyl-1,4-butanedione. However, in the presence of ten equivalents of TFE the yield of 1,4-diphenylcyclohexane-1,4-*cis*-diol was quantitative and no 1,4-diphenyl-1,4-butanedione was recovered. Unlike **1**, the reduction mechanism of **2** is influenced by the presence of a weak non-nucleophilic acid.

When electrolyses of **2** are conducted at more negative potentials, the coulometric values are substantially less than 2 F mol^{-1} of charge. In addition, after disappearance of the dissociative wave corresponding to complete reduction of **2**, at which point the electrolyses were halted, electroactive species are observed at potentials less than −2 V. Electrolyses conducted at −2.2 V in the absence of acid yields a similar product ratio of 98:2 of *cis*-diol and 1,4-diphenyl-1,4-butanedione. The significant difference is that only 1.3 F mol^{-1} of charge is required for complete disappearance of the dissociative wave. However, when the applied potential is shifted more negatively to −2.5 V, three products were identified: *cis*-diol, 1,4-diphenyl-1,4-butanedione and 1,4-diphenyl-1,4-butanediol in a ratio of 54:10:36 as determined by ^{1}H NMR spectroscopy. Most notably at this more negative applied potential, only 0.6 F mol^{-1} of charge is necessary for complete reduction of **2**.

The cyclic voltammetry of an authentic sample of 1,4-diphenyl-1,4-butanedione is shown in Figure 4. The first wave in the reduction of 1,4-diphenyl-1,4-butanedione is scan-rate dependent. At low scan rates the cathodic peak located at −2.0 V is electrochemically irreversible corresponding to 1.3 electrons per molecule. At a scan rate of 20 V s^{-1} the first wave becomes reversible and has a peak height corresponding to 2.0 electrons per molecule. Addition of weak acid results in the first wave becoming totally irreversible

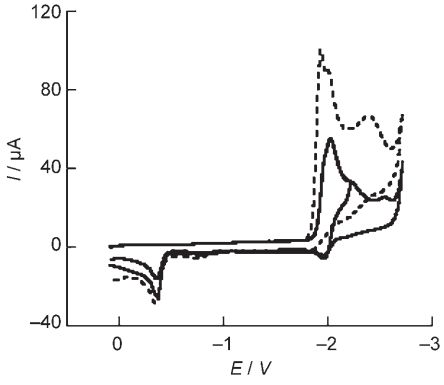

Figure 4. Cyclic voltammograms of 1.9 mM 1,4-diphenyl-1,4-butanedione (**2f**) in the absence (solid line) and presence (dashed line) of five equivalents of TFE in DMF containing 0.1 M TEAP at 0.1 V s^{-1}.

and an increase is observed in the peak height as shown as a dashed line in Figure 4 and consistent with Figure 2.

The acids tested and their corresponding pK_a values in DMF were trifluoroethanol (24.1), acetanilide (22.3), and 2,6-di-*tert*-butylphenol (17.7), which were estimated from their pK_a values in DMSO[20] by applying the relationship pK_a(DMF) = 1.56 + 0.96 pK_a(DMSO).[21] Electrolyses at the first wave consumes 1.3 F mol^{-1} in the absence of acid, but in the presence of 2,6-di-*tert*-butylphenol nearly 4 F mol^{-1} is consumed. The relative electron stoichiometries and voltammetry behavior are consistent with a self-protonation mechanism.[22,23] In other words, 1,4-diphenyl-1,4-butanedione behaves as a weak acid in addition to being an electron acceptor. This has significant implications on the reduction mechanism of **2** (vide infra).

Heterogeneous kinetics and thermochemical parameters: Convolution potential sweep voltammetry was used to evaluate the heterogeneous ET kinetics and pertinent thermochemical parameters for reduction of the O–O bond.[6,9,19,24] Table 2 summarizes the evaluated parameters. Figures S1–S4 of the convolution data are available in the Supporting Information. From the limiting plateau current the diffusion coefficients in 0.1 M TEAP were found to be 7.7×10^{-6} and 7.4×10^{-6} cm^2 s^{-1} for **1** and **2**, respectively. As determined from the α-*E* plots, the evaluated E^o_{diss} and $\Delta G^{\neq}_o$ of **1** and **2** are −0.51 and −0.61 V, and 9.8 and 10.4 kcal mol^{-1}, respectively. Within experimental error, these evaluated parameters are identical. Of significant interest, the E^o_{diss} are substantially less negative than the E_p by at least 0.7 V. This difference is attributed to the large intrinsic barrier that must be overcome to stretch and break the O–O bond as the electron is accepted into the σ* orbital. With knowledge of E^o_{diss}, the standard heterogeneous rate constant (k^o_{het}) was estimated from interpolation of the second-order polynomial fit to the heterogeneous kinetics. The k^o_{het} are extremely low at 7.9×10^{-7} to 3.2×10^{-7} cm s^{-1}, for **1** and **2**, respectively, consistent with a totally irreversible rate-determining electrode reaction characteristic of concerted dissociative ET.[25] The quality of the determined data was finally checked by digital simulation of the dissociative waves. The experimental cyclic voltammograms were adequately reproduced from the data in Tables 1 and 2 based on a concerted dissociative mechanism.

Table 2. Data acquired by convolution sweep potential voltammetry of diphenyl-substituted bicyclic endoperoxides in 0.10 mol L^{-1} TEAP/DMF at 25 °C at a glassy carbon electrode.

	1	**2**
D[a] [cm^2 s^{-1}]	7.7×10^{-6}	7.4×10^{-6}
E^o_{diss} [b] [V]	−0.61	−0.51
log(k^o_{het} [cm s^{-1}])[c]	−6.1	−6.5
$\Delta G^{\neq}_o$[d] [kcal mol^{-1}]	9.8	10.4
λ_{het}[e] [kcal mol^{-1}]	20	20
BDE[f] [kcal mol^{-1}]	19	22
BDFE[g] [kcal mol^{-1}]	11	9.0

[a] Determined from the convoluted limiting current and the known area of the electrode. The area of the electrode was calculated using ferrocene and a diffusion coefficient 1.13×10^{-5} cm^2 s^{-1}. [b] Estimated error is ± 0.10 V and uncorrected for the double layer. [c] Determined by interpolation of the heterogeneous kinetics from a quadratic fit at E^o_{diss}. Estimated error of (logk^o_{het}) ± 0.5 from digital simulation. [d] $\Delta G^{\neq}_o$ determined from the slope of α_{app} vs. E plots and $\Delta G^{\neq}_o = F/[8(d\alpha/dE)]$. [e] $\lambda_{het} = 55.7/r_{eff}$; the calculated radii r_{AB} of 3.6 and 3.7 Å were determined from the Stokes–Einstein equation and the diffusion coefficients; effective radii of 2.8 Å were calculated from $r_{eff} = r_B\,(2r_{AB} - r_B)/r_{AB}$ for both endoperoxides. [f] Calculated from $\Delta G^{\neq}_o = (BDE + \lambda_{het})/4$. [g] Calculated from BDFE = $23.06(E^o_{ORRO^-} - E^o_{diss})$; $E^o_{ORRO^-} = -0.12$ V.

It is worthwhile to compare the convolution parameters from this study with those evaluated for the dialkyl-substituted bicyclic endoperoxides ASC and DASC. The diffusion coefficients and k^o_{het} for ASC and DASC were previously determined to be 1.1×10^{-5} and 6.3×10^{-7} cm^2 s^{-1}, respectively.[6] A comparison of the k^o_{het} values reveals that this parameter is independent of whether the bridgehead substituents are alkyl or phenyl. Furthermore, the $\Delta G^{\neq}_o$ for the diphenylendoperoxides are also within the same range of values 9.6 and 11.0 kcal mol^{-1} for ASC and DASC, respectively. However, the diffusion coefficients for **1** and **2** are considerably smaller, which reflects the additional molecular volume from the bulky phenyl rings. More pertinent, the E^o_{diss} of the diphenyl-substituted endoperoxides are significantly lower than ASC and DASC by 0.5 V. In fact, the E^o_{diss} determined in this study are in agreement with the E^o_{diss} of the anthracene endoperoxide, DPA-O_2, which was found to be −0.56 V versus SCE.[10] The replacement of alkyl groups with phenyl groups has the effect of raising E^o_{diss}. The consequence is that the driving force for ET, $\Delta G_{ET} = 23.06(E^o_{D/D^{\cdot-}} - E^o_{diss})$ is 11.5 kcal mol^{-1} more favorable for the diphenyl-substituted endoperoxides (for which $E^o_{D/D^{\cdot-}}$ could be the reduction potential of an ET donor or the electrode).

The E^o_{diss} is related to the O–O bond dissociation energy (BDE) by the equation $E^o_{diss} = E^o_{ORRO^-} - BDFE/F$ derived from a thermochemical cycle in which $E^o_{ORRO^-}$ is the reduction potential of the distonic radical anion, F is the Faraday constant and the BDFE is the bond dissociation free energy, which is the BDE corrected for entropy (BDFE = BDE − $T\Delta S$).[25,26] The $E^o_{ORRO^-}$ cannot be accurately obtained from cyclic voltammetry due to poor reproducibility, but can be approximated from the standard potential of the cumyl alkoxyl radical which is −0.12 V.[27] By using the above equation, the BDFE for the diphenyl-substituted endoperoxides are 11 and 9 kcal mol^{-1}. Because the entropies of formation are not known, the BDEs were determined by using Savéant's concerted dissociative ET model[18,28] from the experimental $\Delta G^{\neq}_o$ and the expression $\Delta G^{\neq}_o = (\lambda + BDE)/4$, in which λ is the solvent reorganization energy. This last term was calculated from the empirical relation $\lambda = 55.7/r_{AB}$, in which λ is given in kcal mol^{-1} and r_{AB} is the molecular radius given in Å.[29] The molecular radius of each endoperoxide was determined from the Stokes–Einstein equation with the diffusion coefficients determined from the convolution analysis. An effective radius approach was used to more accurately describe the solvation of only the portion of the molecule receiving the charge, while the rest of the molecule acts

to shield the charge from the solvent using the expression $r_{eff}=r_B(2r_{AB}-r_B)/r_{AB}$, in which r_{eff} is the effective radius and r_B is the radius of the charged portion.[28] The charge on the alkoxide fragment was approximated by using the cumyl alkoxide anion resulting in r_{eff} equal to 2.8 Å and leading to λ equal to 20 kcal mol^{-1}. An unknown uncertainty in the intrinsic barrier is the contribution from inner reorganization energy, which is normally assumed to be negligible with respect to the magnitude of the BDE. A summary of this data is included in Table 2.

Using the calculated λ value, the BDEs are calculated to be 19 and 22 kcal mol^{-1}, which are about 8 kcal mol^{-1} lower than for the dialkyl-substituted endoperoxides ASC and DASC. These BDEs represent some of the lowest values ever reported.[30] A similar trend in the BDEs was also observed with the acyclic peroxides bis(triphenylmethyl)peroxide and di-*tert*-butyl peroxide.[19,25] Bis(triphenylmethyl) peroxide has a E^o_{diss} 0.4 V more positive and a BDE 6 kcal mol^{-1} lower than di-*tert*-butyl peroxide. The BDEs of dialkyl peroxides are generally higher than endoperoxides, ranging from 31–37 kcal mol^{-1}, due to the oxygen lone pairs being in a staggered orientation whereas in bicyclic endoperoxides the oxygen lone pairs are eclipsed. The result is that phenyl substituents lower the BDE and make the E^o_{diss} more positive. Thus, not only are **1** and **2** examples of endoperoxides that are easily reduced with reduction potentials of only −0.6 V, they also have rather weak, yet stable O−O bonds.

Reaction mechanisms: The voltammetry of the diphenyl-substituted endoperoxides **1** and **2** is consistent with ET reduction of the O−O bond by a concerted DET mechanism, in which fragmentation occurs simultaneously with electron uptake [Eq. (3)]. For each endoperoxide, the reduction yields the corresponding *cis*-diol as the major product [Eq. (4)]. However, while **1** yields the quantitative formation of the corresponding *cis*-diol, **2** yields a small amount of 1,4-diphenyl-1,4-butanedione in addition to *cis*-diol, which has a dramatic effect on the observed voltammetry. The electrochemical characteristics of **1** are similar to the dialkyl-substituted endoperoxides ASC and DASC in that only a single, broad and electrochemically irreversible cathodic peak is observed. This is in contrast to **2**, which has more elaborate voltammetry like previously studied DPA-O_2 and TPD.[10,12] Unlike these last two endoperoxides, compound **1** is the first example of a diphenyl-substituted endoperoxide that does not exhibit an electrochemically reducible product at a potential more negative than the dissociative wave.

Scheme 3 depicts the proposed ET reduction mechanism of **1**. Recall that the constant potential electrolyses of **1** result in the quantitative formation of the *cis*-diol **1c**, and the consumption of two electrons per molecule in agreement with the proposed mechanism. Upon ET to **1**, the electron is accepted into an σ* orbital associated with the O−O bond, which ruptures in concert, resulting in the formation of the distonic radical anion **1a** with an unpaired electron on one oxygen atom and a negative charge on the other. Subsequently, **1a** generated in the vicinity of the electrode, could be reduced to the dialkoxide **1b** before diffusing away from the electrode, and then protonated in the reaction media or upon workup to yield **1c**. Alternatively, **1a** could be protonated by the reaction media, notably upon addition of an acid, to yield the alkoxyl radical **1d**, which could be further reduced and subsequently protonated to yield **1c**. At this time, it is not known how to experimentally differentiate the fate of **1a** between these two possibilities. Nonetheless, the outcome is the same resulting in quantitative formation of *cis*-diol **1c**. The reduction potentials of **1a** and **1d** are not accurately known, and difficult to determine directly by cyclic voltammetry due to poisoning of the electrode surface. However, the reduction potentials of **1a** and **1d** can be approximated by the cumyl alkoxyl radical with a known standard potential of −0.12 V versus SCE in DMF.[27] Since the E_p of **1** is located at a potential more negative than −1.2 V, the reductions of **1a** and **1d** are predicted to be thermodynamically favorable by at least 23 kcal mol^{-1}.

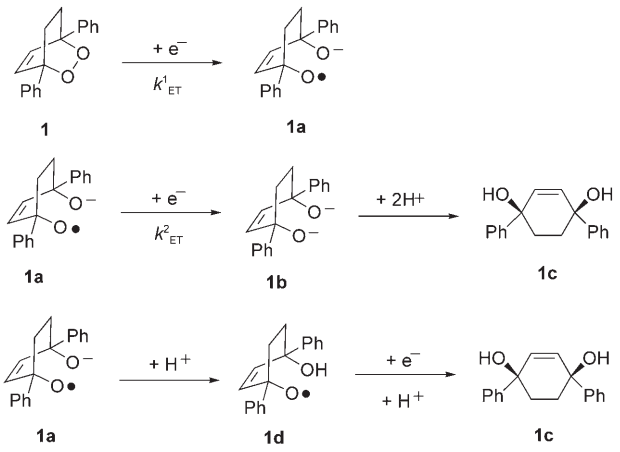

Scheme 3. The heterogeneous ET mechanism proposed for the reduction of **1**.

The mechanism postulated for **1** also applies to the formation of *cis*-diol in the reduction of **2**. However, the mechanism of **2** must also account for the formation of 1,4-diphenyl-1,4-butanedione, the observation of the dip after the dissociative wave, the affect of excess weak acid on the voltammetry, and the potential dependence on the electron stoichiometry. The isolation of 1,4-diphenyl-1,4-butanedione, a product with a molecular weight less than the parent endoperoxide, suggests the mechanism must involve a competition between reduction and fragmentation of the distonic radical anion **2a**.

Scheme 4 illustrates the proposed mechanism for the heterogeneous reduction of **2** in the absence of an added weak acid. To account for the experimental observations, a propagating radical-anion chain mechanism is postulated.[12] Initially, **2** is reduced by concerted dissociative ET to generate the distonic radical anion **2a**, which could react similarly to **1a** (Scheme 3) to yield the *cis*-diol **2c**. However, in addition to reduction at a potential of −1.5 V, **2a** also reacts by a

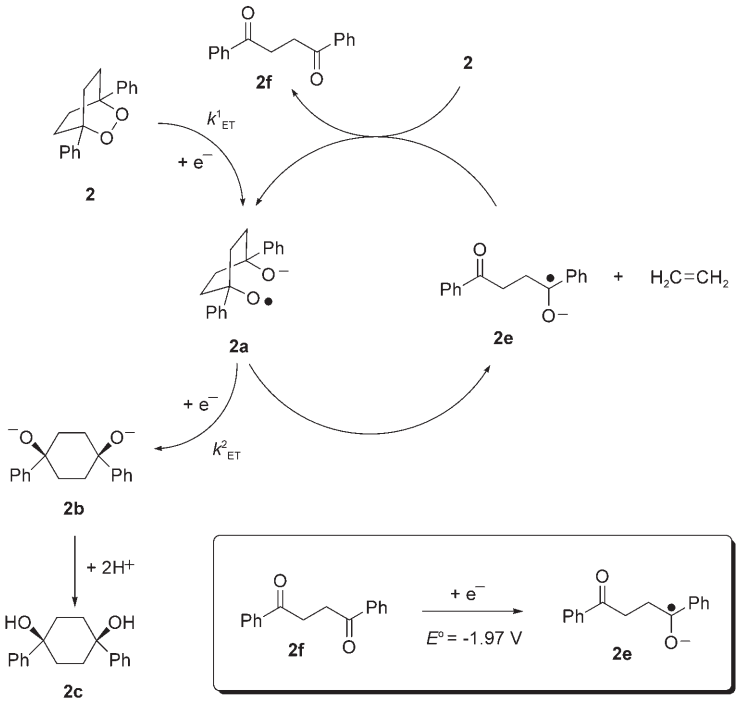

Scheme 4. The propagating radical-anion chain mechanism proposed for the ET reduction of **2**. In the lower box the one-electron reduction of 1,4-diphenyl-1,4-butadione (**2e**) highlights the potential dependence of the mechanism, and the ability of **2e** to behave as a homogeneous ET catalyst at a reduction potential of −1.97 V.

competitive β-scission fragmentation to yield **2f** and ethylene via formation of the ketyl radical **2e**. Note that **2e** is also a radical anion, but the spin and charge are no longer spatially separated. Also note that in Scheme 4 the fragmentation is shown to be a concerted process, although it could be stepwise; however, no evidence of products resulting from a stepwise fragmentation were observed. The radical anion **2e**, formed as a consequence of the fragmentation, is a potential homogeneous ET donor capable of reducing **2**. The standard potential of 1,4-diphenyl-1,4-butanedione (**2f**) was measured to be −1.97 V versus SCE. This is 1.5 V more negative than the E^o_{diss} of **2**. Therefore, the homogeneous reductions of **2** and **2a** are both thermodynamically favorable by over 30 kcal mol^{-1}.

Beyond the dissociative wave, **2** displays an oxidative dip rather than a gradual decrease in current dictated exclusively by diffusion. This feature in the voltammograms, most noticeable at slower scan rates, is a consequence of the competitive β-scission fragmentation from **2a**. The lower current value reflects a decrease in the concentration of **2** diffusing towards the electrode. In fact, the oxidative dip is the result of **2** being reduced homogeneously, in competition with the electrode reduction. The dip occurs just before the standard potential of **2f** at −1.97 V. At this potential, the equilibrium shifts towards an increase in the concentration of radical anion **2e**. Because of a build-up in the concentration of **2e** in the vicinity of the electrode, diffusing **2** approaching the electrode is intercepted by **2e** and reacts by a homogeneous ET to generate **2a** and **2f**. Any **2f** at the electrode surface could be reduced to the radical anion **2e** and react with more incoming **2**.

Now we consider the presence of excess weak acid. It could affect the reduction mechanism of **2** in two ways (Scheme 5). First, it could protonate the distonic radical anion **2a**. Evidence for this comes from the electrolyses of **2** in the presence of excess weak acid at potentials positive to the standard potential of 1,4-diphenyl-1,4-butanedione, and within the potential range of the dissociative wave (−1.4 to −1.8 V). In the presence of 10 mM TFE, **2f** was not detected in a measurable amount; the only isolated product was the *cis*-diol. Protonation of **2a** must hinder the fragmentation from competing with reduction from the electrode. Therefore, the β-scission

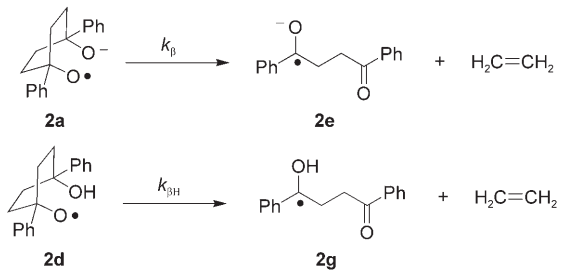

Scheme 5. β-scission fragmentation of the distonic radical anion **2a** and the corresponding alkoxyl radical resulting from protonation **2d**. Experimental evidence suggests **2a** fragments faster than the analogous alkoxyl radical **2d** as observed from electrolysis experiments.

fragmentation of the resulting alkoxyl radical **2d** must be slower than fragmentation of **2a**, supporting the notion that both charge and spin affect the rates of radical-anion rearrangements.[2,3] The second way excess weak acid could affect the reduction mechanism is by protonating the radical anion **2e**. This would prevent homogeneous ET reactions between **2e** and **2**.

Further support for these conclusions comes from recent studies of DPA-O_2 and TPD.[10,12] In both studies an electroactive product with a standard potential more negative than the dissociative wave results from fragmentation of the distonic radical anion in competition with heterogeneous reduction. The voltammetry of DPA-O_2 lacks a dip, and no

evidence of a generated radical-anion, ET donor was found.[10] In contrast, in the study of TPD an oxidation dip is observed, and the mechanism involves the formation of a benzophenone radical anion.[12]

All that remains is to account for the potential dependence of the electron stoichiometry in the reduction of **2**. In electrolyses conducted in the vicinity of the dip and the dissociative wave, which are at potentials between −1.4 V and −2.0 V, 2 F mol^{-1} of charge is consumed. At −2.2 V the reduction consumes 1.3 F mol^{-1} of charge, and at −2.5 V only 0.6 F mol^{-1} of charge. The possible reasoning for this last observation is as follows. As seen in Scheme 4, **2** is initially reduced to the distonic radical anion **2a** and fragments to a small extent to yield the radical anion **2e**, which can transfer an electron to **2** resulting in the formation of **2f** and another molecule of **2a**. The result is a catalytic radical-anion chain reaction.[12,31,32] For each **2a** generated, one molecule of **2f** can be potentially formed depending primarily on the competition between fragmentation and ET reduction of **2a**. In the reduction mechanism, 1,4-diphenyl-1,4-butanedione takes on the role of a homogeneous catalyst, which propagates the chain reaction. However, **2f** is not a robust catalyst; 1,4-diphenyl-1,4-butanedione also undergoes a competing self-protonation mechanism between the radical anion **2e** and the starting neutral molecule **2f**. The α-protons of **2f** are acidic enough to protonate **2e**.[22] However, the charge consumption is even less at −2.5 V compared to −2.2 V, because at the more negative applied potential both aryl ketones are reduced to yield the dianion, which inhibits the self-protonation mechanism. The dianion can act as a two-electron donor to propagate the reaction mechanism, but also leads to the formation of 1,4-diphenyl-1,4-butanediol on protonation as illustrated in Scheme 2. With the second heterogeneous ET to **2e** likely to be faster than the homogeneous proton transfer from **2f**, the self-protonation mechanism is not as competitive at −2.5 V and the observed electron consumption is considerably less than **2** (see Table 1).

Thermochemical cycle: The distonic radical anion **2a** undergoes a fragmentation able to compete with the heterogeneous ET reduction from the electrode, whereas the analogous species **1a** does not. Both endoperoxides have similar E_p (Table 1) so the driving force for the ET to the distonic radical anions are the same. Therefore, this discrepancy in distonic radical-anion reactivity must be an intrinsic property related to the molecular structure, the only difference between **1a** and **2a** is the absence of the double bond in the latter. To reconcile these observations, a thermochemical cycle (Scheme 6) has been devised.

The thermochemical cycle identifies three contributing factors to the driving force of the distonic radical-anion fragmentation reactivity:[4] 1) the thermodynamic stability of the delocalized distonic radical anion as reflected by the oxidation potential, 2) the fragmentation of the biradical, and 3) the stability of the localized radical anion as measured by the reduction potential.

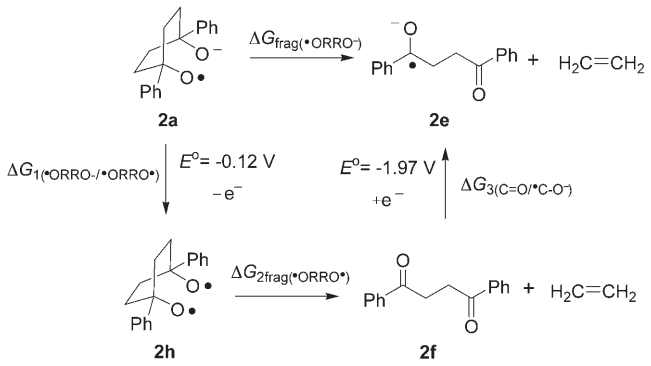

Scheme 6. Thermochemical cycle for evaluating the driving force for fragmentation of the distonic radical anion **2a**.

It should be noted that no attempt has been made to account for any interaction between the radical and anion portions of the distonic radical anion. Table 3 summarizes the various thermochemical values for the diphenyl- and dialkyl-substituted endoperoxides and corresponding reactive intermediates. The overall driving force for the fragmentation of the distonic radical anion $\Delta G_{frag(\cdot ORRO^-)}$ is given by Equation (5).

Table 3. Thermodynamic data for fragmentation of structurally similar neutral biradicals and distonic radical anions.[a]

	1	**2**	ASC	DASC
$\Delta H^o_{f(ROOR)}$ [b]	53.8	12.60	−18.8	−62.3
$\Delta S^o_{f(ROOR)}$ [b]	79.2	85.19	56.8	62.0
$\Delta G^o_{f(ROOR)}$	30.2[c]	−12.8	−35.7[c]	−80.8
BDFE	11.0	9.0	22.4[d]	22.4[d]
$\Delta G^o_{f(\cdot ORRO\cdot)}$ [e]	41.2	−3.8	−13.3	−58.4
$\Delta G^o_{f(diketone)}$ [b]	na[k]	−73.4	na[k]	−141.7
$\Delta G_{2frag(\cdot ORRO\cdot)}$ [f]	na	−73.1	na	−86.8
$\Delta G_{1(\cdot ORRO^-/\cdot ORRO\cdot)}$ [g]	−2.8	−2.8	−5.3	−5.3
$\Delta G_{3(C=O/(\cdot C-O^-)}$ [h]	−45.4[i]	−45.4[i]	−74[j]	−74[j]
$\Delta G_{frag(\cdot ORRO^-)}$	na	−30.5	na	−18.1

[a] Values at 298 K in kcal mol^{-1} except for $\Delta S^o_{f(ROOR)}$ in cal K^{-1} mol^{-1}. [b] Group addivity estimates from the NIST Structures and Properties Database, reference [33]. [c] *E*stimated from reference [33] by using hydrocarbon models without O atoms and corrected using values from reference [34]. [d] BDFE = 23.06($E^o_{\cdot ORRO^-}$-E^o_{diss}); E^o_{diss} from reference [10]. [e] $\Delta G^o_{f(\cdot ORRO\cdot)}$ = BDFE + $\Delta G^o_{f(ROOR)}$. [f] Free energy for fragmentation of the biradical: $\Delta G_{2frag(\cdot ORRO\cdot)} = \Delta G^o_{f(diketone)} + \Delta G^o_{f(ethylene)} - \Delta G^o_{f(\cdot ORRO\cdot)}$; $\Delta G^o_{f(ethylene)} = -3.5$ kcal mol^{-1} calculated from reference [33]. [g] $\Delta G_{1(\cdot ORRO^-/\cdot ORRO\cdot)} = FE_{1(\cdot ORRO^-/\cdot ORRO\cdot)}$; $E_{1(\cdot ORRO^-/\cdot ORRO\cdot)}$ estimated from values for the cumyloxy ($E°$ = −0.12 V) and *tert*-butoxyl ($E°$ = −0.23 V) radical; reference [27]. [h] $\Delta G_{3(C=O/(\cdot C-O^-)} = -FE_{3(C=O/(\cdot C-O^-)}$; [i] $E_{3(C=O/(\cdot C-O^-)} = -1.97$ V this work. [j] $E_{3(C=O/(\cdot C-O^-)} = -3.2$ V from reference [2]. [k] Group addivities not available (na) for the carbonyl group in the *cis*-diketones.

$$\Delta G_{frag(\cdot ORRO^-)} = \Delta G_{1(\cdot ORRO^-/\cdot ORRO\cdot)} + \Delta G_{2frag(\cdot ORRO\cdot)} - \Delta G_{3(C=O/(\cdot C-O^-)} \quad (5)$$

The $\Delta G_{1(\cdot ORRO^-/\cdot ORRO\cdot)}$ and $\Delta G_{3(C=O/(\cdot C-O^-)}$ values are easily calculated from the oxidation potentials of the distonic radi-

cal anion and the reduction potentials of the ketones, respectively, from electrochemically measurements or related literature values.[27] However, for $\Delta G_{2frag(^{\cdot}ORRO^{\cdot})}$ we require the Gibbs energies of formation of the biradical and the values for the products assuming the fragmentation yields only the diketone and ethylene according to Equation (6).

$$\Delta G_{2frag(^{\cdot}ORRO^{\cdot})} = \Delta G^{o}_{f(diketone)} + \Delta G^{o}_{f(ethylene)} - \Delta G^{o}_{f(^{\cdot}ORRO^{\cdot})} \quad (6)$$

The Gibbs free energies for the biradicals $\Delta G^{o}_{f(^{\cdot}ORRO^{\cdot})}$ were calculated from the free energies for the endoperoxides determined by using group addivity estimates,[33,34] and experimentally determined BDFEs according to $\Delta G^{o}_{f(^{\cdot}ORRO^{\cdot})} = BDFE + \Delta G^{o}_{f(ROOR)}$. Unfortunately, group addivities are not readily available for the carbonyl groups in the *cis*-diketones so we could not obtain $\Delta G_{frag(^{\cdot}ORRO^{-})}$ for **1** and ASC. However, we were able to obtain a complete thermochemical data set for **2** and DASC, and also the free energy of formation $\Delta G^{o}_{f(^{\cdot}ORRO^{\cdot})}$ for all four biradicals. By using the thermochemical cycle we not only provide some quantitative information regarding the reactivity of distonic radical anions, but it also allows us some insight into the relationship between distonic radical anions and the analogous oxygen-centered biradicals.

In Table 3 a comparison of the thermochemical parameters of the endoperoxides and biradicals reveal some interesting trends. The enthalpy $\Delta H^{o}_{f(ROOR)}$ increases on substitution of the alkene moiety and the phenyl rings in the order DASC < ASC < **2** < **1**. A change from the alkane to the alkene functionality raises $\Delta H^{o}_{f(ROOR)}$ by 42 kcal mol^{-1} and replacement of the alkyl bridgehead substituents with phenyl rings by 74 kcal mol^{-1}. The entropy $\Delta S^{o}_{f(ROOR)}$ is generally consistent with all values being positive, the endoperoxides with phenyl rings having slightly larger values. The result is that the $\Delta G^{o}_{f(ROOR)}$ parallels $\Delta H^{o}_{f(ROOR)}$ with DASC < ASC < **2** < **1** with values ranging from −81 to 30 kcal mol^{-1}. The $\Delta G^{o}_{f(^{\cdot}ORRO^{\cdot})}$ has the same trend, with values ranging from −58 to 41 kcal mol^{-1}, again with all values favorable except for **1**.

The $\Delta G_{2frag(^{\cdot}ORRO^{\cdot})}$ for the biradicals of **2** and DASC are favorable with values of −73.1 and −86.8 kcal mol^{-1}. These results are consistent with the precedence for β-scission fragmentation on thermolysis and photolysis of saturated bicyclic endoperoxides.[35,36] From Equation (5) the calculated $\Delta G_{frag(^{\cdot}ORRO^{-})}$ values are −30.5 and −18.1 kcal mol^{-1} for **2** and DASC, respectively. The thermodynamic results suggest that both of these distonic radical anions should fragment; yet, no fragmentation products were observed in the previous study of DASC.[6] The reason for this lack of observation has to do with the electrode potential. The overpotentials for reduction of the distonic radical anions of **2** and DASC are calculated to be −23 and −18 kcal mol^{-1}. Therefore, fragmentation of **2a** is predicted to easily compete with the heterogeneous ET reduction by −7 kcal mol^{-1}, whereas the DASC analogue is on par.

Another contributing reason for the absence of fragmentation from the distonic radical anion of DASC may be due to a lack of charge stabilization. Stevenson et al. have reported various studies on the ring opening of substituted cyclopropyl and cyclobutyl radical-anion ketones to their distonic radical anions.[2,3] The distonic radical anion **2a** fragments to a localized radical anion as generalized in Equation (2), which is the reverse general direction studied by them.[2,3] They reasoned that the fragmentation of ketyl radical anions is slower than from analogous carbon radicals due to resonance stabilization of the negative charge into the phenyl ring. Our results support their findings. As illustrated in Scheme 5, we observed that the alkoxyl radical **2d** undergoes a slower fragmentation to **2g** than the fragmentation of the distonic radical anion **2a** to **2e**, since the negative charge in **2e** is stabilized into the phenyl ring.

So why was **1a** not observed to undergo a β-scission fragmentation even though resonance stabilization would be possible in the ketyl product? As stated earlier, group addivity values are not readily available for the carbonyl groups in the *cis*-ketones so we could not calculate $\Delta G_{frag(^{\cdot}ORRO^{-})}$ for **1** and ASC. It is possible that the energy barrier for fragmentation is just too great to overcome. In the case of **2a**, there is conformational mobility, which favors β-scission fragmentation from a chair conformation. However, the double bond in **1a** restricts the distonic radical anion to a twist conformation.[12]

At this time, the rate constants for β-scission fragmentation of the distonic radical anions **1a** and **2a** (and protonated forms **1d** and **2d** and the biradicals) have not been reported. As a first approximation, the β-scission fragmentation of the cumyl alkoxyl radical is used as an analogous fragmentation, which has a known rate constant 7×10^{5} s^{-1}.[37] This value represents the upper limit for the fragmentation rate constant for **1a** and the lower limit for **2a**. Therefore, the observation of 1,4-diphenyl-1,4-butanedione in the heterogeneous reduction of **2** can serve as a kinetic probe to estimate the rate constant of the second heterogeneous ET to **2a**. As seen from the reduction potential of the cumyl alkoxyl radical of −0.12 V versus SCE for **2a** (and the protonated form **2d**), the distonic radical anion is generated at potentials more negative than −1.4 V. From the measured product ratio of 98:2 (**2c**/**2f**) and the estimate of 7×10^{5} s^{-1} for k_{β}, the first-order equivalent of the heterogeneous ET rate constant is 3×10^{7} s^{-1}.

Conclusion

Among the qualitative observations resulting from this study, we found that the β-scission fragmentation of the neutral hydroxy alkoxyl radical **2d** and distonic radical anion **2a** are not the same, the latter occurring faster due to resonance stabilization of charge into the phenyl ring. Thus, we provide evidence that the fragmentation rates of radical anions can be considerably different than the fragmentation rates for analogous neutral biradicals. At present, there is a general lack of information on the heterogeneous kinetics to various electrogenerated intermediates, most notably carbon radicals, which typically result from the reduction of alkyl

halides.[18] By exploiting the competition between the fragmentation and heterogeneous reduction of electrogenerated intermediates,[10,13] we have begun to create a library of radical-anion clocks.

Dissociative ET theory was applied to the activation-driving force relationships to obtain unknown thermochemical information. Most interestingly, the evaluated BDEs of diphenyl-substituted endoperoxides are extremely low. The reasoning for this observation is attributed to the eclipsing interaction of the electron lone pairs on the oxygen atoms and the presence of phenyl rings in the bridgehead positions. Several studies have demonstrated that ET to O–O bonds is non-adiabatic,[6,13,27,38] possibly due to violation of the Born–Oppenheimer approximation at the transition state during ET to the O–O bond.[39] This electronic barrier is manifested as a kinetic contribution as observed by the low magnitude of k^{o}_{het}. This kinetic barrier is the reason why endoperoxides with rather weak covalent bonds of 20 kcal mol^{-1} are thermally stable with melting points in excess of 140 °C.

This study also highlights an unprecedented radical-anion chain mechanism initiated by the concerted DET reduction of a bicyclic endoperoxide. Upon reduction of **2**, the distonic radical anion **2a** undergoes a β-scission fragmentation in competition with direct reduction from the electrode. The fragmentation results in the formation of ethylene and the ketyl radical anion **2e**, which can homogeneously reduce **2** and propagate the radical-anion chain mechanism. Although a competing self-protonation mechanism involving 1,4-diphenyl-1,4-butanedione as well as the presence of other weak non-nucleophilic acids can protonate the distonic radical anion **2a**, thus decreasing the efficiency of the radical-anion chain reaction, the significance of this unusual mechanism should not be understated. Recently we reported, in collaboration, the first example of a competition between a concerted and stepwise DET mechanism for antimalarial G3-factor endoperoxides,[40] which potentially opens up an alternative mode of action. Our present results reveal another novel mode of reactivity initiated by ET that could have implications not only on understanding the reduction mechanism of naturally occurring endoperoxides, but could also be useful in the design and synthesis of antimalarial prodrug models.[41]

Experimental Section

Materials: *N*,*N*-Dimethylformamide (DMF) was distilled over CaH_2 under a nitrogen atmosphere at reduced pressure. Tetraethylammonium perchlorate (TEAP) from Fluka was recrystallized three times from ethanol and stored under vacuum. Flash chromatography was performed with silica gel 60 (230–400 mesh ASTM) from EM science. Fractions were developed in the chosen eluant with Kieselgel 60 F_{254} thin-layer chromatography (TLC) plates and viewed by ultraviolet or visible light or iodine staining. Methanol and ethanol were freshly distilled from magnesium. Toluene was freshly dissolved from sodium and benzophenone. Photooxygenation reactions were performed in solutions of spectroscopic grade dichloromethane (Caledon) and benzene (EM Science). Other solvents and reagents not specified were used without purification and obtained from Aldrich.

Instrumentation: Melting points were recorded on an Electrothermal 9100 capillary melting point apparatus and were corrected. UV/Vis spectra were recorded on a Varian Cary 100 Bio UV/Vis spectrometer. IR spectra were recorded on a Bruker Vector 33 FT-IR spectrometer on NaCl plates or in a solution cell. The IR frequencies were reported in cm^{-1} and followed by a letter (w, m, or s) designating the relative strength of the IR stretches as weak, medium, or strong. NMR spectra were recorded on a Varian Mercury spectrometer and reported in ppm. ^{1}H and ^{13}C NMR spectra were recorded at 400.1 and 100.6 MHz, respectively, with $CDCl_3$ as the solvent. Spectra are reported in ppm versus tetramethylsilane ($\delta = 0.00$ ppm) for ^{1}H NMR and $CDCl_3$ ($\delta = 77.00$ ppm) for ^{13}C NMR spectra. Mass spectrometry was performed on a MAT 8200 Finnigan high-resolution mass spectrometer by electron impact (EI) and by chemical ionization (CI) with isobutane.

Synthesis: 1,4-Diphenyl-1,4-butanedione was synthesized by Friedel–Crafts acylation by reacting succinyl chloride with benzene. 1,4-Diphenyl-1,4-butanediol was synthesized by reduction of 1,4-diphenyl-1,4-butanedione with excess sodium borohydride. The endoperoxides were synthesized according to literature procedures with slight modifications.[14,15]

Compound 1: 1,4-Diphenyl-2,3-dioxabicyclo[2.2.2]oct-5-ene (**1**) was purified by flash chromatography using hexanes and dichloromethane (3:2) and recrystallized from a mixture of diethyl ether/dichloromethane as white needles (48 %). M.p. 145–146 °C; ^{1}H NMR ($CDCl_3$, 400 MHz): $\delta =$ 1.96–2.09 (m, 2H), 2.59–2.72 (m, 2H), 6.88 (s, 2H), 7.35–7.46 (m, 6H), 7.51–7.58 ppm (m, 4H); ^{13}C NMR ($CDCl_3$, 100 MHz): $\delta = 29.68$, 78.37, 125.94, 128.24, 128.37, 136.32, 139.20 ppm; IR (CCl_4): $\tilde{\nu} = 3090$ (w), 3063 (s), 3033 (m), 2972 (m), 2935 (s), 2860 (w), 1496 (w), 1449 (s), 1370 (s), 1317 (w), 1184 (w), 1063 (m), 933 (m), 908 (m), 696 (s), 679 cm^{-1} (m); MS EI: *m*/*z* (%): 264 (1) [M^+], 233 (20), 232 (100), 154 (8), 141 (11), 115 (15), 105 (34), 91 (17), 77 (33); MS CI: *m*/*z* (%): 265 (8) [M^++1], 249 (10), 248 (38), 233 (20), 232 (100), 218 (12), 206 (18), 105 (27), 77 (8); exact mass: 264.1156 (calcd 264.1150).

Compound 2: 1,4-Diphenyl-2,3-dioxabicyclo[2.2.2]octane (**2**) was recrystallized from diethyl ether/methylene chloride to yield white needles (63 %). M.p. 193–195 °C; ^{1}H NMR ($CDCl_3$, 400 MHz): $\delta = 2.19$–2.35 (m, 4H), 2.42–2.58 (m, 4H), 7.25–7.39 (m, 6H), 7.40–7.46 ppm (m, 4H); ^{13}C NMR ($CDCl_3$, 100 MHz): $\delta = 31.69$, 78.24, 124.90, 127.68, 128.16, 141.97 ppm; IR (CCl_4): $\tilde{\nu} = 3090$ (w), 3064 (m), 3032 (m), 2969 (s), 2936 (s), 1496 (m), 1449 (s), 1437 (w), 1339 (m), 1119 (m), 1047 (w), 964 (w), 908 (m), 696 (s), 675 cm^{-1} (m); MS: *m*/*z* (%): 266 (25) [M^+], 249 (32), 238 (9), 234 (11), 233 (19), 232 (33), 146 (9), 144 (9), 130 (40), 117 (14), 105 (100), 91 (16), 77 (57); exact mass: 266.1301 (calcd 266.1302).

Electrochemistry: Cyclic voltammetry was performed either on a Perkin–Elmer PAR 283, or 263A potentiostat interfaced to a personal computer equipped with PAR 270 electrochemistry software. Experiments were performed with a three-electrode arrangement placed in a water-jacket cell stored in an oven at 110 °C. It was placed in a copper Faraday cage, purged with a continuous flow of high-purity argon and connected to a cooling bath maintained at 25 °C throughout the entire experiment. The electrolyte was added to the cell followed by DMF (25 mL) and a half-inch magnetic stir bar. The solution was bubbled with argon to expel oxygen from the solution. The working electrode was a 3 mm diameter glassy carbon rod (Tokai, GC-20) sealed in glass tubing. Prior to use it was polished on a polishing cloth with diamond paste, rinsed and sonicated in 2-propanol for 10 min and finally dried with a stream of cool air. The working electrode was activated by cycling 25 times between 0 and −2.8 V versus SCE at a scan rate of 0.2 V s^{-1}. The counter electrode was a 1 cm^2 Pt plate. The reference electrode was a silver wire immersed in a glass tube with a sintered end containing 0.10 M TEAP in DMF. After each experiment, it was calibrated against the ferrocene/ferricinium couple at 0.475 V versus KCl saturated calomel electrode (SCE) in DMF.

Heterogeneous product studies: Constant potential electrolyses were performed with a Perkin–Elmer PAR 263A potentiostat. The working electrode was a 12 mm tipped glassy carbon rotating-disk electrode (EDI101) with a CTV101 speed control unit from Radiometer Analytical. The counter electrode was a platinum wire immersed in a glass frit containing 2 mm layer of neutral alumina. The reference electrode was a silver wire contained in a sintered glass frit and stored in an electrolyte solution

before use. A 3 mm glassy carbon electrode was used to probe the experiment. After cell setup and activation of the probe electrode, the electrolyte solution was pre-electrolyzed at a potential several hundred millivolts short of the solvent discharge. A voltammogram of the background was recorded. The substrate was added to the solution and voltammograms recorded. Electrolysis were performed at a constant potential, and routinely halted to probe the decrease in current with added charge. A plot of current by charge added to the cell allowed the required charge for complete electrolysis to be determined. Electrolyses were continued until the monitored peak current was reduced to the initial background. Afterwards, dilute acetic acid (10 mL) was added to the cell and the contents extracted with dichloromethane (3×15 mL). The organic extract was washed with brine (3×20 mL) and water (20 mL), dried over sodium sulphate and filtered; the solvent evaporated on a rotary evaporator. Trace solvent was removed by vacuum pump. The mass balance was recorded and the products analyzed. Electrolyses were performed with minimum concentrations of 1 mM endoperoxide.

Heterogeneous electrolysis products: From the electrolysis of 1,4-diphenyl-2,3-dioxabicyclo[2.2.2]oct-5-ene (**1**) was recovered 1,4-diphenyl-cyclohex-2-ene-*cis*-1,4-diol in 100% yield; ^{1}H NMR ($CDCl_3$, 400 MHz): $\delta=$ 1.61 (brs, 2H), 1.93–1.97 (m, 2H), 2.15–2.22 (m, 2H), 6.08 (s, 2H), 7.23–7.31(m, 2H), 7.33–7.41(m, 4H), 7.49–7.56 ppm (m, 4H), alcohol peak verified by deuterium exchange; ^{13}C NMR ($CDCl_3$, 100 MHz): $\delta=$36.38, 72.45, 125.29, 127.33, 128.27, 134.42, 145.83 ppm; IR (NaCl): $\tilde{\nu}$3348 (brs), 3078 (w), 3057 (w), 3024 (m), 2930 (s), 2920 (s), 2850 (w), 1652 (w), 1597 (w), 1446 (w), 1048 (m), 976 (m), 759 cm^{-1} (w); MS: *m*/*z* (%): 266 (7) [M^+], 238 (21), 220 (18), 146 (100), 133 (24), 105 (30), 91 (7), 77 (19); exact mass: 266.1309 (calcd 266.1307). Note that prolonged exposure of the diol in $CDCl_3$ results in dehydration to *p*-terphenyl likely due to trace acid. *p*-Terphenyl was measured to have a standard potential of −2.298 V versus SCE and not observed during the electrolysis experiments.

From the electrolysis of 1,4-diphenyl-2,3-dioxabicyclo[2.2.2]octane (**2**) at the peak potential was recovered 1,4-diphenyl-cyclohexane-*cis*-1,4-diol in 98% yield; ^{1}H NMR ($CDCl_3$, 400 MHz): $\delta=$1.74 (brs, 2H), 2.14 (brs, 8H), 7.23–7.30 (m, 2H), 7.31–7.38 (m, 4H), 7.44–7.51 ppm (m, 4H), alcohol peak verified by deuterium exchange; ^{13}C NMR ($CDCl_3$, 100 MHz): $\delta=$35.43, 72.64, 125.18, 127.25, 128.39 ppm (1 phenyl carbon atom is unaccounted); IR (NaCl): $\tilde{\nu}=$3386 (brs), 3089 (w), 3060 (w), 3030 (w), 2946 (s), 2869 (w), 1559 (w), 1541 (w), 1495 (m), 1447 (w), 1051 (m), 976 (m), 762 (s), 700 cm^{-1} (s); MS: *m*/*z* (%): 268 (1) [M^+], 250 (8), 233 (3), 222 (14), 221 (11), 145 (14), 135 (78), 134 (100), 131 (23), 120 (37), 105 (67), 91 (16), 77 (28); exact mass: 268.1464 (calcd 268.1463).

Acknowledgements

This work was financially supported by the Natural Sciences and Engineering Research Council of Canada, the Government of Ontario (PREA) and the University of Western Ontario. D.C.M. thanks the Ontario Government for an OGSST postgraduate scholarship. Doug Hairsine is thanked for performing the mass spectroscopic measurements.

[1] Z. V. Todres, *Organic Ion Radicals: Chemistry and Applications*, Marcel Dekker, New York, **2003**.
[2] J. P. Stevenson, W. F. Jackson, J. M. Tanko, *J. Am. Chem. Soc.* **2002**, *124*, 4271–4281.
[3] J. M. Tanko, J. P. Phillips, *J. Am. Chem. Soc.* **1999**, *121*, 6078–6079.
[4] M. Chahma, X. Li, P. Phillips, P. Schwartz, L. E. Brammer, Y. Wang, J. M. Tanko, *J. Phys. Chem. A* **2005**, *109*, 3372–3382.
[5] J. M. Tanko, X. Li, M. Chahma, W. F. Jackson, J. N. Spencer, *J. Am. Chem. Soc.* **2007**, *129*, 4181–4192.
[6] R. L. Donkers, M. S. Workentin, *Chem. Eur. J.* **2001**, *7*, 4012–4020.
[7] M. S. Workentin, R. L. Donkers, *J. Am. Chem. Soc.* **1998**, *120*, 2664–2665.
[8] D. C. Magri, R. L. Donkers, M. S. Workentin, *J. Photochem. Photobiol. A* **2001**, 29–34.
[9] R. L. Donkers, M. S. Workentin, *J. Phys. Chem. B* **1998**, *102*, 4061–4063.
[10] R. L. Donkers, M. S. Workentin, *J. Am. Chem. Soc.* **2004**, *126*, 1688–1698.
[11] R. L. Donkers, J. Tse, M. S. Workentin, *Chem. Commun.* **1999**, 135–136.
[12] D. L. B. Stringle, M. S. Workentin, *Chem. Commun.* **2003**, 1246–1247.
[13] D. C. Magri, M. S. Workentin, *Org. Biomol. Chem.* **2003**, *1*, 3418–3429.
[14] K. Gollnick, G. O. Schenck, in *1,4-Cycloaddition Reactions* (Ed.: J. Hamer), Academic Press, New York, **1967**, pp. 255–343.
[15] Y. Takahashi, K. Wakamatsu, S. Morishima, T. Miyashi, *J. Chem. Soc. Perkin Trans. 2* **1993**, 243–253.
[16] D. J. Coughlin, R. S. Brown, R. G. Salomon, *J. Am. Chem. Soc.* **1979**, *101*, 1533–1539.
[17] W. Adam, H. J. Eggelte, *J. Org. Chem.* **1977**, *42*, 3987–3988.
[18] J.-M. Savéant, *Adv. Phys. Org. Chem.* **2000**, *35*, 117–192.
[19] S. Antonello, M. Musumeci, D. D. M. Wayner, F. Maran, *J. Am. Chem. Soc.* **1997**, *119*, 9541–9549.
[20] F. G. Bordwell, *Acc. Chem. Res.* **1988**, *21*, 456–463.
[21] F. Maran, D. Celadon, M. G. Severin, E. Vianello, *J. Am. Chem. Soc.* **1991**, *113*, 9320–9329.
[22] C. Amatore, G. Capobianco, G. Farnia, G. Sandonà, J.-M. Savéant, M. G. Severin, E. Vianello, *J. Am. Chem. Soc.* **1985**, *107*, 1815–1824.
[23] A. B. Meneses, S. Antonello, M. C. Arévalo, F. Maran, *Electrochim. Acta* **2005**, *50*, 1207–1215.
[24] The background subtracted voltammograms are transformed to sigmoidal-shaped *i-E* curves by use of the convolution integral and the experimental current *i*: $I_{lim}=\pi^{-1/2}\int_0^t \frac{i(u)}{(t-u)^{1/2}}du$. The limiting current, I_{lim}, at the plateau of the sigmoidal-shaped *i-E* curves is diffusion-controlled and define as $I_{lim}=nFAD^{1/2}C^*$ in which *n* is the overall electron consumption, *A* is the electrode area, *D* is the diffusion coefficient, and C^* is the substrate concentration.
[25] F. Maran, D. D. M. Wayner, M. S. Workentin, *Adv. Phys. Org. Chem.* **2001**, *36*, 85–166.
[26] D. D. M. Wayner, V. D. Parker, *Acc. Chem. Res.* **1993**, *26*, 287–294.
[27] R. L. Donkers, F. Maran, D. D. M. Wayner, M. S. Workentin, *J. Am. Chem. Soc.* **1999**, *121*, 7239–7248.
[28] J.-M. Savéant, *Adv. Electron Transfer Chem.* **1994**, *4*, 53–116.
[29] H. Kojima, A. J. Bard, *J. Am. Chem. Soc.* **1975**, *97*, 6317–6324.
[30] Y.-R. Luo, *Handbook of Bond Dissociation Energies in Organic Compounds*, CRC, Boca Raton, Florida, **2003**.
[31] J.-M. Savéant, *Acc. Chem. Res.* **1980**, *13*, 323–329.
[32] J. Pinson, J.-M. Savéant, *J. Am. Chem. Soc.* **1978**, *100*, 1506–1510.
[33] S. E. Stein, R. L. Brown, Y. A. Mirokhin, in *NIST Structures and Properties Database and Estimation Program*, Gaithersburg, MD, **1991**.
[34] S. W. Benson, in *Free Radicals, Vol. 2*, 2nd ed., Wiley, New York, **1976**.
[35] W. Adam, *Acc. Chem. Res.* **1979**, *12*, 390–396.
[36] W. Ando, *Organic Peroxides*, Wiley, New York, **1992**.
[37] D. V. Avila, C. E. Brown, K. U. Ingold, J. Lusztyk, *J. Am. Chem. Soc.* **1993**, *115*, 466.
[38] S. Antonello, F. Formaggio, A. Moretto, C. Toniolo, F. Maran, *J. Am. Chem. Soc.* **2001**, *123*, 9577–9584.
[39] L. J. Butler, *Annu. Rev. Phys. Chem.* **1998**, *49*, 125.
[40] F. Najjar, C. André-Barrès, C. Lacaze-Dufaure, D. C. Magri, M. S. Workentin, T. Tzèdakis, *Chem. Eur. J.* **2007**, *13*, 1174–1179.
[41] P. M. O'Neill, P. A. Stocks, M. D. Pugh, N. C. Araujo, E. E. Korshin, J. F. Bickley, S. A. Ward, P. G. Bray, E. Pasini, J. Davies, E. Verissimo, M. D. Bachi, *Angew. Chem.* **2004**, *116*, 4289–4293; *Angew. Chem. Int. Ed.* **2004**, *43*, 4193–4197.

Received: November 5, 2007
Published online: January 25, 2008

